# Scalar Transport in an Oscillatory Velocity Field Evolving Under Boundary Noise

Vena Pearl Boñgolan
Department of Computer Science, College of Engineering
University of the Philippines Diliman
Quezon City
bongolan@dcs.upd.edu.ph

Jinquiao Duan
Department of Applied Mathematics
Illinois Institute of Technology
Chicago, IL 60616
duan@iit.edu

George Skountrianos
Department of Statistics
The University of Chicago
Chicago, IL 60637
trekvana@aol.com

## ABSTRACT

This study extends previous work on the space-averaged salinity of a gravity current evolving under an assumed sinusoidal shear-flow with noise in the boundary. The shear flow produces an oscillatory salinity profile for the current, and this was previously observed to have high-amplitude oscillations for high-frequency shear-flows, regardless of the noise, with or without noise. One finding in this extended study is that it happens even for low-frequency shear flows, and various frequencies are being studied. These oscillations attain several relative maxima when plotted against the frequency, suggesting resonance.

Experiments with the variance of the noise (interpreted as its strength) affects most the salinity profile of currents evolving under Lévy colored noise,and results suggest decreasing transport as noise strength increases, and the relationship is linear. All oscillations were observed to get damped as the experiments progress, but Lévy colored noise tends to hasten this damping as noise strength increases.

A new metric to measure the effect of boundary noise is also being developed, wherein we normalize the effects of the noise by subtracting the averaged salinity from the non-homogenous, deterministic base case, giving a 'noise effect'. Wiener white and colored noises, as well Lévy white noise, help the transport process, resulting in an increased 'signal' or average salinity. Uniquely, Lévy colored noise initially helps the signal, but pretty soon 'eats' the signal, suggesting decreased transport.

## Categories and Subject Descriptors

J.2 [**Physical Science and Engineering**]: Miscellaneous; I.6.3 [**Computing Methodologies**]: Simulation and Modeling—*applications to ocean gravity currents*

## 1. INTRODUCTION



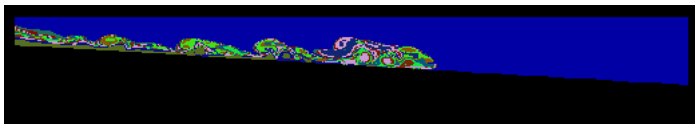

**Figure 1: Gravity current with Neumann boundary conditions at time 6375 seconds**

Gravity or density currents are the flow of one fluid within another caused by the temperature or density difference between the fluids [1], e.g., the more dense and salty Mediterranean waters flowing into the relatively fresh waters of the North Atlantic through the Strait of Gibraltar. They are an important component of the thermohaline circulation [2], which in turn is important in climate and weather studies. Figure 1 shows the temperature distribution of a simulated gravity current, from a previous experimental set-up used in [3]. The color-density plot ranges from red (coldest) to blue (warmest). The horizontal distance is ten kilometers, and the depth of the water column ranges from 400 meters on the left (inlet), and one kilometer on the right (outlet), over a constant slope. In this paper, however, the passive scalar is salinity, instead of temperature.

In a previous paper, [4], we investigated the effects of boundary noise in the inlet conditions of the scalar transport equation driven by an assumed sinusoidal shear-flow. This was motivated by several observations, like the seasonal variability of the Red Sea overflow (a source of salty, dense water flowing into the Gulf of Aden), [5]. Taking a slightly different approach, we modeled this observed variability by the addition of a noise term in the flux boundary conditions at the inlet.

In this study, we investigate the effects of the frequency of the oscillating shear flow $\frac{1}{\tau}$, the strength of the noise ($\sigma$), and the distribution which produced the noise ($\alpha$). Wiener white and colored (time-correlated) noises were used, the latter being closer to what is observed in nature [6]. We also made use of a more general class of processes, Lévy processes, which are generally non-Gaussian in distribution, and may have infinitely many jumps in finite time, subject to the integrability condition.

Following McNamara and Wiesendfeld's [7] approach to the system as a 'blackbox', we define the inputs to the sys-

tem as the triple $(\alpha, \tau, \sigma)$, respectively: the stability index for the Lévy processes ($\alpha$), the frequency of the sinusoidal shear-flow ($f = \frac{1}{\tau}$, where $\tau$ is the period) and the *scale parameter* ($\sigma$), which is usually called standard deviation for processes with a Gaussian distribution, and which we take here to be the strength of the noise. This noise strength features in the boundary condition $\frac{\partial S}{\partial n} = F(z) + \epsilon_n$. The 'output' or signal we are observing is the salinity at time $t$, or S(x,z,t), which we average over the spatial domain. We will interchangeably refer to this as the space-averaged or simply averaged salinity.

In the case of non-homogenous Neumann, $\epsilon_n = 0$. In the experiments, $\epsilon_n$ may be Wiener or Lévy, white or colored.

# 2. SCALAR TRANSPORT EQUATION WITH RANDOM BOUNDARY FLUXES

Young et al. [8] modeled advection-diffusion in the oscillatory, sheared-velocity field of an internal wave, by assuming $u = \beta t \cos(\tau * t)$, or a variant with sinusoidal vertical structure, $u = u_0 \cos(mz)\cos(\tau * t)$. We likewise assume a known velocity field in the scalar transport equation.

We consider a passive scalar (also called **tracer**) $S = S(x, z, t)$, where $S$ may be taken to be temperature, salinity or concentration of a chemical specie. Assuming the velocity field $u(x, z, t)$ is known from the fluid momentum equations ($u$ is divergence-free and no-slip on boundary),

$$S_t + u \cdot \nabla S = \kappa \Delta S, \ (x, z) \in D \tag{1}$$

where $D = [0, 1] \times [0, 1]$, and $\kappa > 0$ is the salute diffusivity.

We supplement this linear transport equation with the following boundary conditions

$$\frac{\partial S}{\partial n} = F(z) + \text{noise, on inlet boundary , x=0} \tag{2}$$

$$\frac{\partial S}{\partial n} = 0 \text{ on rest of boundary} \tag{3}$$

where $F(z)$ is the mean tracer or passive scalar flux. In the case of Wiener white noise, $\frac{\partial S}{\partial n} = F(z) + \dot{W}_t$, where $W_t$ is a Brownian motion defined in a probability space.

A form for the solution is known, using a theorem of Da Prato and Zabczyk [9]. If we let A be the linear (in S) operator

$$A = -u \cdot \nabla - \kappa \Delta, \ (x, z) \in D \tag{4}$$

then the equation has the form

$$S_t = AS \tag{5}$$

and we write the boundary conditions as a vector Y

$$Y = \begin{pmatrix} F(z) + \dot{W}_t \\ 0 \end{pmatrix}, \tag{6}$$

we may let operator $\gamma$ define the boundary conditions as:

$$\gamma S = Y. \tag{7}$$

Here, we will just assume that A generates a $C_0$ semigroup of operators X(t), $t \geq 0$. A proper proof will require verification of the requirements of the Lumer-Philipps theorem.

If we designate as

$$\mathcal{N}(Y) = \phi \tag{8}$$

where

$$A(\lambda - \phi) = 0 \tag{9}$$

that is, $\mathcal{N}$ is the solution operator of the above eigenvalue problem, then we write the solution as:

$$S = X(t)S_0(x, z) + (\lambda - A)\int_0^t X(t - s)\mathcal{N}(Y)ds \tag{10}$$

## 2.1 The Numerical Model and Simulations

We made use of a finite-element diffusion-convection-reaction solver developed at Clemson University by Prof. Vince Ervin. The domain is a $16x16$ triangularization of the square $[0, 1]x[0, 1]$. This solves the transport equation for a tracer $S(x, z, t)$ on a rectangular domain, under flux (Neumann) boundary condition.

$$S_t + v \cdot \nabla S + qS = \nabla(\kappa \cdot \nabla S), \tag{11}$$

where $\kappa > 0$ is the salute diffusivity, and $v$ is a given function for velocity of the bulk flow. For our problem, $q$ is zero (no reaction term).

Here, the diffusivity constant $\kappa = .01$ was assumed constant throughout the domain, chosen to 'slow-down' the diffusion process and allow the gravity current to evolve during our simulation time.

Young et al. [8] assumed velocity fields like $u = \beta t \cos(\tau * t)$ or $u = u_0 \cos(mz)\cos(\tau * t)$. In this study, we likewise assumed an oscillatory shear flow $v$ in the $x$ (downstream) direction, zero in the vertical (z) direction, The x-component has the form

$$v = .5 * z * \cos(\tau * t) * scaling, \tag{12}$$

where scaling ($presently = 75$) is used to control the speed of the current.

Time-stepping was by the backward-Euler method.

In the simulations following, we assumed $F = 1$ in the boundary condition $F(z)+$noise. Thus, the comparison case is a non-homogenous Neumann boundary condition, which could represent the average flux for the tracer, which we later perturb with noise.

At each time-step, the tracer was averaged as

$$Average = \frac{\int_{triangle} S dx dz}{\text{area of triangle}} \tag{13}$$

where the integral is over each triangle in the spatial discretization. The values from all triangles in the domain were then averaged, giving the average value for the entire current at $time = t$.

The initial conditions for the salinity are shown in Figure 2. We might imagine a high-salinity body of water enters the domain at the origin, and will flow along the positive x-axis. The starting salinity profile is highest at the bottom of the current, and decreases along the y-axis.

Figure 3 shows the salinity distribution at $t = 400$, which shows a quick diffusion over the domain, as the current evolves.

Figure 4 plots the averaged scalar value for the entire domain at time $t$, i.e., $S(x, z, t)$, for a current evolving with the constant flux $F = 1$. A close inspection of the graph shows this happens in an oscillatory manner,due to the oscillatory shear flow. This is how all the salinity distributions behave, with or without noise in the boundary. Figure 5 shows a 'close-up' view.

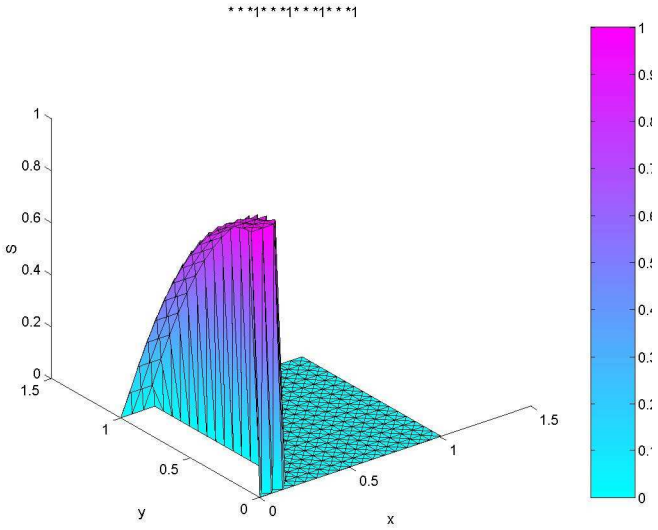


**Figure 2: Initial salinity distribution**

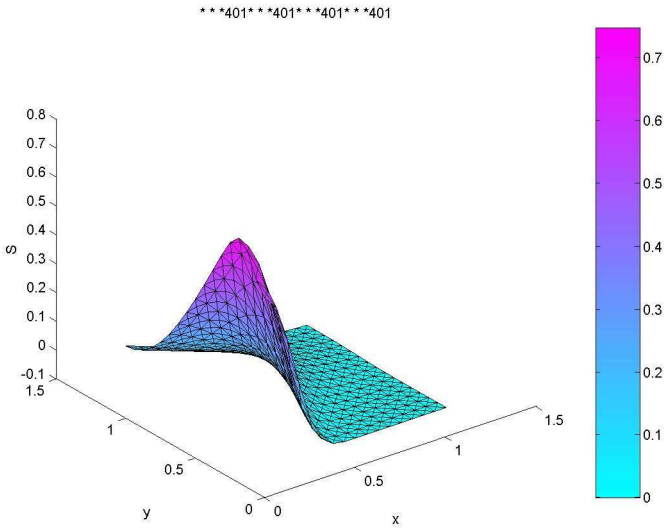


**Figure 3: Initial salinity distribution**

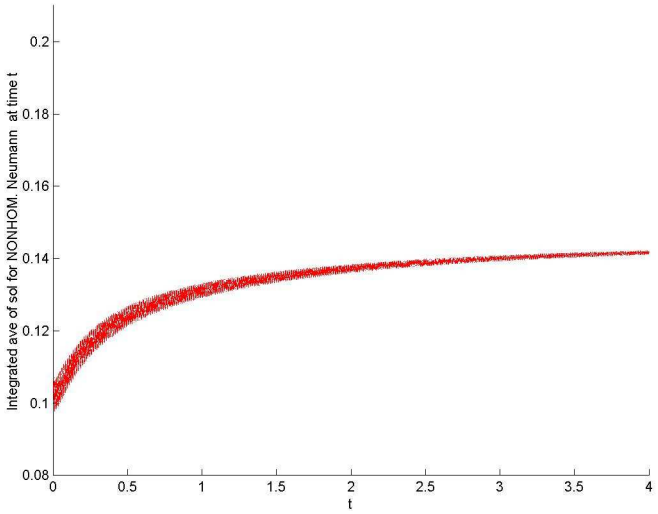


**Figure 4: space-averaged salinity without noise**

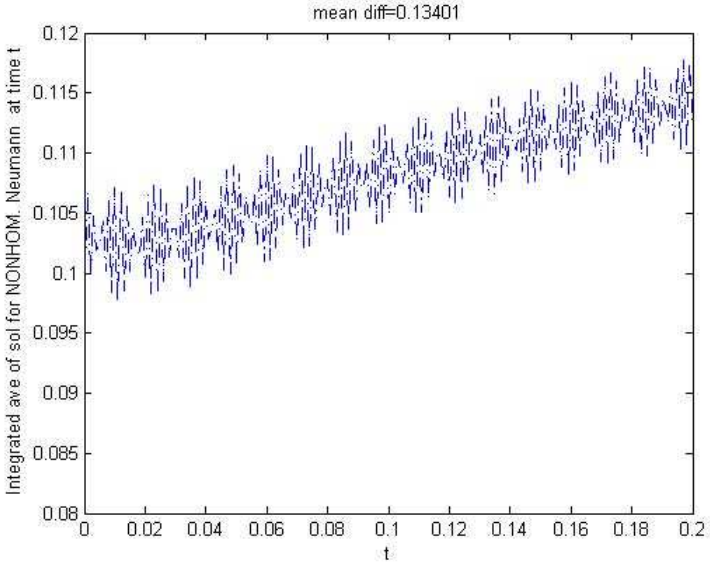


**Figure 5: Close-up of the curve at t=0.2**

## 2.2 Summary of Noise Processes

We now summarize the more detailed discussion on noises given in [4].

**Wiener White Noise:**

Wiener white noise $\dot{W}_t(u)$ is the formal derivative of a Brownian motion $W_t$, and may be regarded as a solution of the simplest linear stochastic differential equation

$$\dot{W}_t(u) = \frac{dW_t}{dt} \tag{14}$$

Usually called Gaussian white noise, we will refer to it here as Wiener white noise, to distinguish it from the noise from an $\alpha$-stable Lévy processes could also include white noise with a Gaussian distribution (when $\alpha = 2$).

**Lévy White Noise:**

There is a more general class of noises which may also be taken to be 'white' in the sense they are uncorrelated in time, but their distribution need not be Gaussian. A Lévy process $L_t, (t \geq 0)$ taking values in $\mathbb{R}^d$ is a stochastic process having stationary and independent increments, and we assume that $L_0 = 0$ almost everywhere.

Lévy processes $L_t$ are defined in terms of their characteristic function, viz:

$$\mathbb{E}(e^{i(u,L_t)}) = e^{tg(u)} \tag{15}$$

where

$$g(u) = i(b,u) - \frac{1}{2}(u,au) + \tag{16}$$

$$\int_{\mathbb{R}^d - \{0\}} (e^{i(u,y)} - 1 - i(u,y)\chi_{0<|y|<1}(y))\mathbf{m}(dy). \tag{17}$$

This is the Lévy -Khintchine formula, and from here we see that Lévy processes encompass familiar processes, e.g., if $a = \mathbf{m} = 0$, we have $L_t = bt$ which is deterministic motion in a straight line, where b is the velocity of motion, or the *drift*. Similarly, if $a \neq 0$, $\mathbf{m} = 0$, then $L_t$ is a Brownian motion with drift, since the formula gives us the characteristic function of a Gaussian random variable with mean $tb$ and covariant matrix $ta$.

With a choice of measure $\mathbf{m}$, and jump sizes $h_i$ (which may be variable), we may generate Poisson processes, aside from Brownian motion which may have drift.

For our numerical simulations, we use $\alpha$-stable Lévy motions defined in Janicki and Weron [10]. See also [11].

Taking a particular form of the Lévy -Khintchine formula, let $L_t$ be a stochastic process having independent increments, and we also assume that $L_0 = 0$ with probability of one. Now, we assume $L_t - L_s \sim G_\alpha((t-s)^{\frac{1}{\alpha}}, \beta, 0)$ for any $0 \leq s < t < \infty$.

$G_\alpha(\sigma, \beta, \mu)$ is the general symbol for an $\alpha$-stable random variable is, whose characteristic function is given by

$$\log \phi(\theta) = -\sigma^\alpha |\theta|^\alpha (1 - i\beta sgn(\theta)\tan(\alpha\pi/2)) + i\mu\theta \tag{18}$$

where $\alpha \in (0,1) \bigcup (1,2]$ is the index of stability; $\beta \in [-1,2]$ is the skewness; $\sigma \in \mathbb{R}_+\sigma$ is the scale parameter (simply standard deviation when $\alpha = 2$); and $\mu \in \mathbb{R}$ is the shift (mean) of the distribution, .

We transcribed the computer simulation provided by Janicki and Weron for the class of processes $G_\alpha(1,0,0)$. When $\alpha$ is 2, the resulting motion is Brownian, and the distribution is in fact Gaussian. Away from $\alpha = 2$, the distribution goes away from being Gaussian, providing a very interesting class of motions which include Cauchy motion (when $\alpha = 1$), and Lévy motion when $\alpha$ is any other number in (0,2).

**Colored Noises:**

A colored noise $\eta_t(u)$ is a solution of a linear Ornstein-Uhlenbeck stochastic equation

$$\frac{\partial \eta}{\partial t} = -b\eta + a\frac{dW_t}{dt} \tag{19}$$

where $\frac{dW_t}{dt} = \dot{W}_t$ is Wiener white noise. $\eta_t(u)$ has time-correlated covariance, and is thus used as a model for colored noise. This was solved via Milstein's Method, see [6].

We model Lévy colored noise similarly, except that the term $\frac{dW_t}{dt}$ replaced by Lévy white noise $\frac{dL_t}{dt}$, so

$$\frac{\partial \nu}{\partial t} = -b\nu + a\frac{dL_t}{dt} \tag{20}$$

Janicki and Weron generalized the Milstein method to include Lévy processes in Chapters 6 and 8 of [10].

## 2.3 Review of Previous Results

In [4], comparisons were made among currents evolving under deterministic boundary conditions (non-homogenous Neumann) and with a stochastic term added to the boundary, viz: Wiener white and colored noises and Lévy white and colored noises.

Both Wiener noises (white and colored), and white Lévy noise all had the effect of enhancing the transport process, producing a current that was considerably more saline. These three boundary conditions gave a higher average value for the tracer, $\bar{S} = .08$, compared to .06 for the deterministic base case. Colored Lévy noise, gave the same ending averaged value as the deterministic case, $\bar{S} = .06$.

However, it was Lévy colored noise which showed sensitivity to the stability parameter $\alpha$, as this determines the actual nature of the distribution, with $\alpha = 2$ being Gaussian, $\alpha = 1$ being Cauchy, all others, we call Lévy.

Another finding is that uncorrelated (white) noises act very similarly, i.e., white Wiener noise had similar effects on the current as white Lévy noises, suggesting that time-correlation is more important in distinguishing the effects of noise, rather than the distribution of the processes that produced the noise.

In the experiments on the frequency of the velocity of the shear flow, a higher-frequency flow $f = \frac{3}{\tau}$ showed noticeable increases in the amplitude of the oscillations or variability of the averaged scalar values, with the biggest increase seen with colored Lévy noise (almost doubled). However, this increase in transport is only local, and oscillatory, hence did not affect the average values for the tracer.

## 2.4 Results and Discussion

In this paper, we extend the previous experiments by varying the stability index $\alpha$ (or varying the distribution of the noise), the frequency of the sinusoidal shear-flow $\frac{1}{\tau}$, and the scale parameter $\sigma$, the strength of the noise.

### *2.4.1 Varying the frequency of the shear-flow, $f = \frac{1}{\tau}$*

Recall the x-component of the velocity vector for our shear flow: $v = .5 * z * \cos(\tau * t) * scaling$, with the y-component

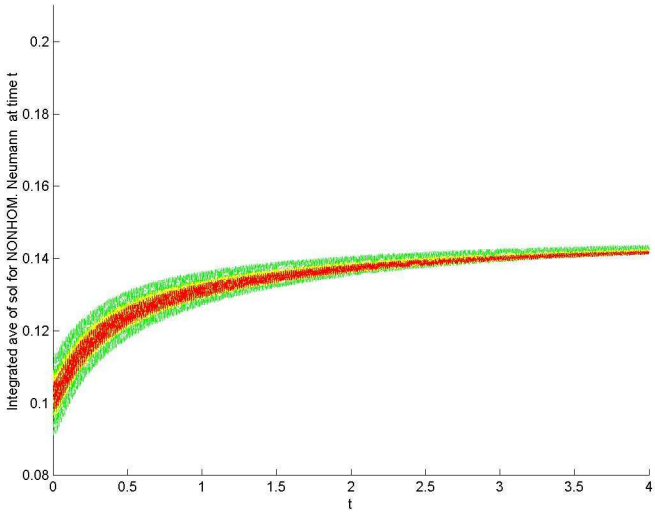


**Figure 6: averaged salinity at higher frequencies of the sinusoidal flow red (f=1) yellow (f=2) green (f=4)**

being zero. We take $\tau = 1$ as the 'normal' period, giving the normal frequency, $f = 1$.

Previously, the experiments with a higher-frequency shear-flow (e.g., $f = \frac{3}{\tau}$) resulted in noticeable increases in the amplitude of the oscillations or variability of the averaged scalar values, with the biggest increase seen with colored Lévy noise, about twice the normal amplitude.

Figure 6 shows the increasing amplitudes of the oscillations as we go to higher frequencies, i.e., from $f = 1$ to $f = 4$. This effect is observed regardless of the noise, with or without noise. Similar effects for low-frequency shear-flows were also observed.

Next we subtract the average salinities for normal frequency from that when frequency is halved, and might refer to this as the 'frequency effect'. Here we show results for longer runs, 12000 time-steps. Most cases show this difference to be oscillatory, decaying with time. Interestingly, Figure 7, for Levy colored noise, reveals decay to a small number, then increases again.

Figure 8 graphs the average oscillation for several values of $\tau$, and we see relative maxima occurring at several places, at different values.

### 2.4.2 *Sensitivity to the noise-strength, or scale parameter $\sigma$*

We interpret the scale parameter $\sigma$ as the strength of the noise, and the finding is that it affects most the current with colored Lévy Noise. Figure 9 shows the averaged salinities decreasing (suggesting decreased transport) as $\sigma$ goes from 1 (red) to 2 (cyan). No other noise process differentiates the $\sigma$ values. Figure 10 show the salinities for Wiener colored noise, and has the graphs all on top of each other, suggesting robustness in the transport process with respect to the strength of the white noises (Wiener and Lévy) and Wiener colored noise.

An interesting result was obtained when we again calculated the frequency effect (subtract averaged salinites with a

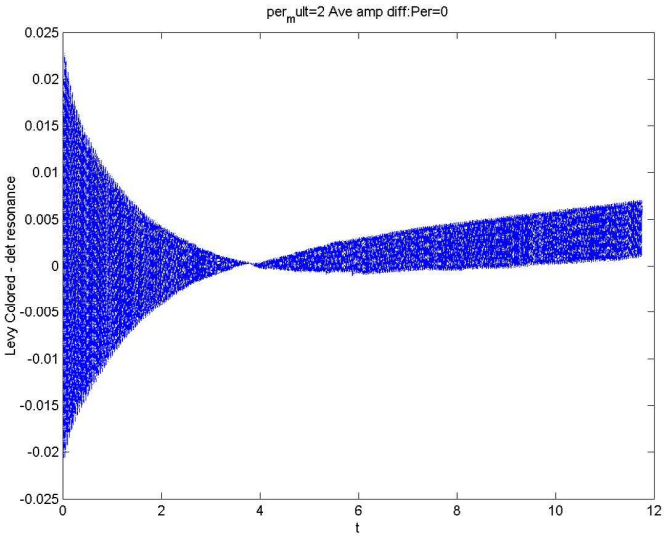


**Figure 7: half-frequency salinity less standard frequency salinity**

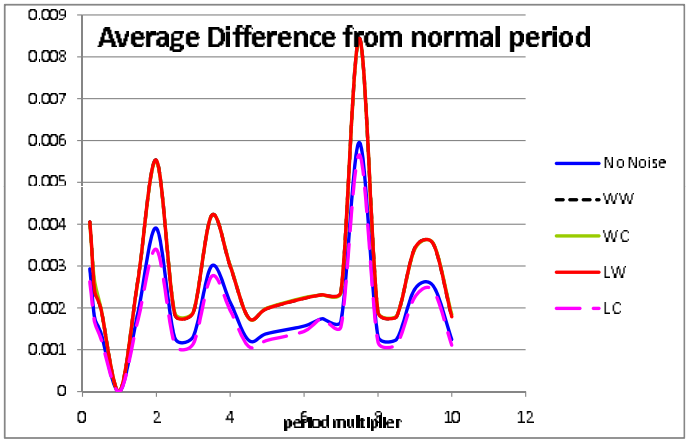


**Figure 8: plot of average amplitude difference against period $\tau$**

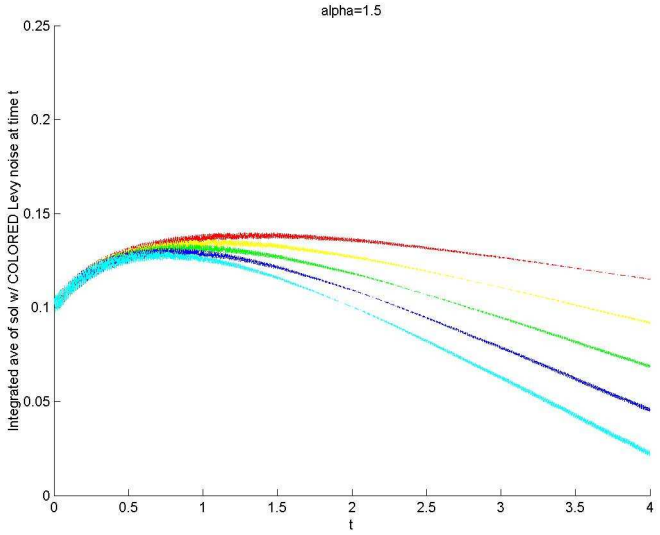


**Figure 9: $\sigma$ =1 (red) $\sigma$=1.25 (yellow) $\sigma$=1.5 (green) $\sigma$=1.75 (blue) $\sigma$=2 (cyan)**

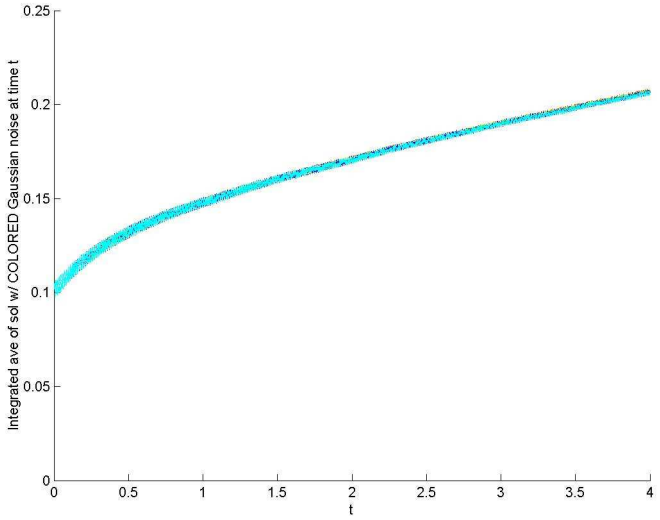


**Figure 10: $\sigma$ =1 (red) $\sigma$=1.25 (yellow) $\sigma$=1.5 (green) $\sigma$=1.75 (blue) $\sigma$=2 (cyan)**

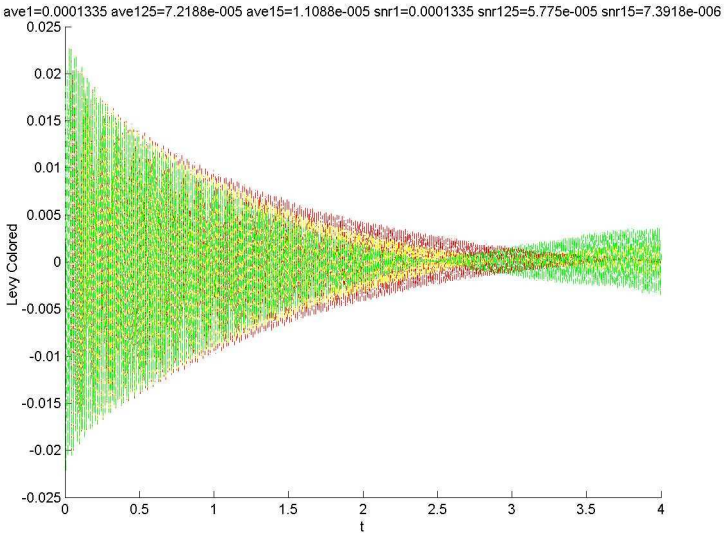


**Figure 11: half frequency-normal frequency, $\sigma$ =1 (red) $\sigma$=1.25 (yellow) $\sigma$=1.5 (green)**

normal frequency from the averages for a halved frequency). Figure 11 shows the results for Lévy colored noise, where the difference gets damped to a small number, then increases again, and increasing the strength of the noise hastens this damping. Repeating this experiment with other noises shows the curves all on top of each other, i.e., the frequency effect is not sensitive to Lévy white and Wiener white and colored noises.

### *2.4.3 Measuring the Effects of boundary noise*

This is a metric we developed, where we attempt to measure the effects of boundary noise as the gravity current evolves, by subtracting the averaged salinity of a current evolving without noise from the averaged salinity of a current evolving with noise, and refer to this as the 'noise effect'.

Figure 12 shows the noise effect for a current evolving with white Lévy noise; it shows a continuous, almost linear in time, increase in salinity. We might say that white Lévy noise 'helps the signal', with signal being taken as the averaged salinity; we have similar results for Wiener white and colored noises.

Figure 13 shows the noise effect for colored Lévy noise, and we see that, initially, it 'helps' the salinity (helps the transport), but pretty soon, it 'eats' the signal (or less transport).

As with the other experiments, the noise effect was subjected to varying stability parameter $\alpha$, variance $\sigma$ and frequency $f = \frac{1}{\tau}$.

**Effect of the distribution of Lévy noise processes :index of stability $\alpha$**

The $\alpha$ parameter determines the distribution of the Lévy noise processes, with $\alpha = 2$ being Gaussian, $\alpha = 1$ being Cauchy. We calculate the noise effect, and we see this affects more the current evolving with colored Lévy noise, as shown in Figure 14, with the signal being 'eaten-up' faster as we move closer to Gaussianity in the distribution. White Lévy

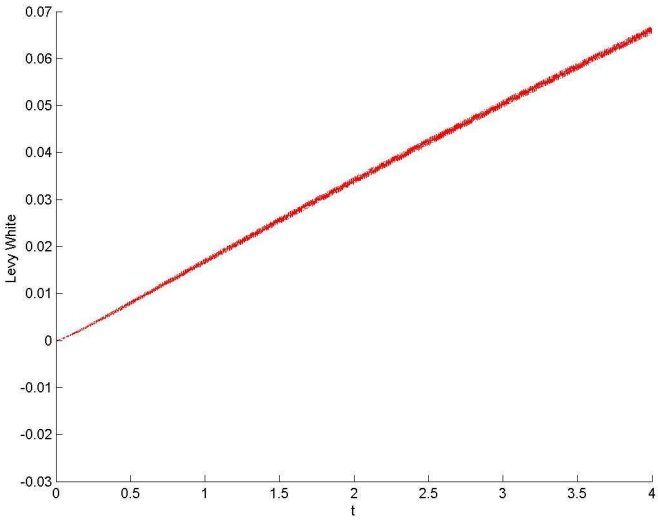


**Figure 12: averaged salinity with Lévy White noise - non-homogenous Neumann (base case)**

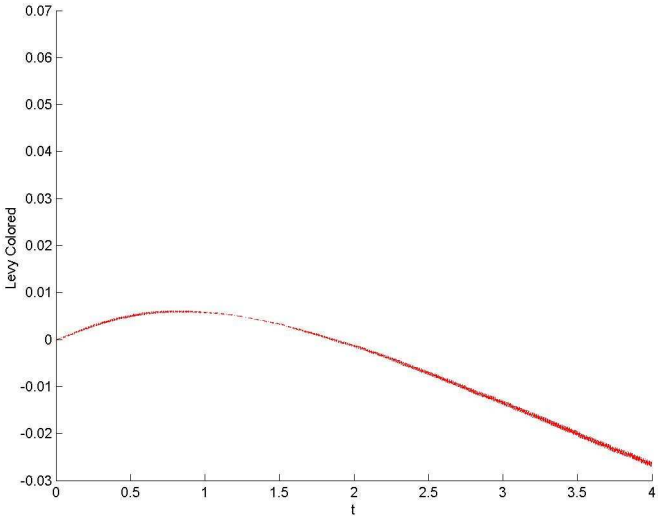


**Figure 13: averaged salinity with Lévy Colored noise - non-homogenous Neumann (base case)**

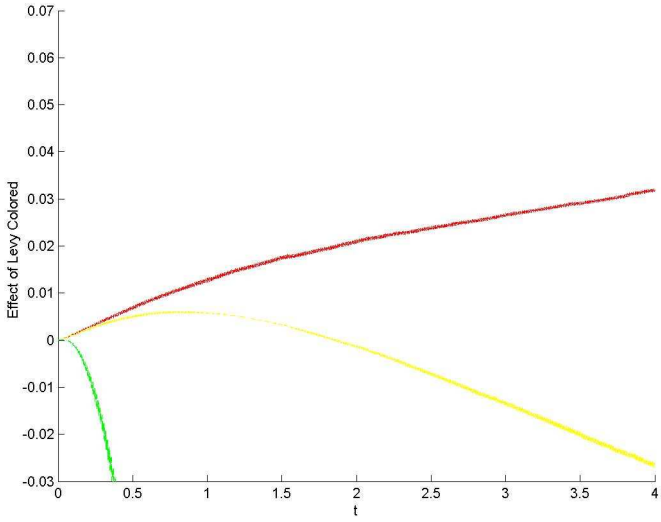


**Figure 14: averaged salinity with Lévy Colored noise - non-homogenous Neumann (base case); $\alpha$=1.25 red $\alpha = 1.5$ yellow $\alpha = 1.75$ green**

noise does not have this effect, and the graphs are again all on top of each other, suggesting that the noise effect is robust with respect to the distribution of the Lévy process that produced the noise.

### Sensitivity to the frequency of the shear flow

What happens to the noise effect is similar to Figures 12 and 13, with all noises helping the signal, except Lévy colored noise, which eats the signal. Figure 15 shows the now familiar increase in amplitude with increasing frequency. regardless of the noise process used.

### Varying the strength of the noise $\sigma$ affects most the current with Lévy colored noise

Similar to Figure 9, Figure 16 shows the noise effect broken up by the variance, and the signal is eaten up faster with increasing variance or strength of the noise. Comparisons of salinity distributions of the four noises, all at the same variance, show results similar to Figures 12 and 13 combined.

## 3. CONCLUSIONS

Interpreting the space-averaged salinity as a signal in a blackbox system, we saw that varying the period of the shear-flow $\tau$ suggested resonance in the salinity profile, which we directly interpret as resonance in the transport equation, similar to what has been observed in plasmas. An intriguing finding is that the average salinity seemed insensitive to the strength of Wiener white and colored noises, as well as Lévy white noise, but Lévy colored noise is very sensitive to this parameter.

A suggested possible explanation is that the parameter variations done in the experiments might not have been large enough to fully test the typical time scales that we expect to get into play, viz., the diffusion time scale, velocity field period and correlation time. Refinements to the experiments could be the subject of future work.

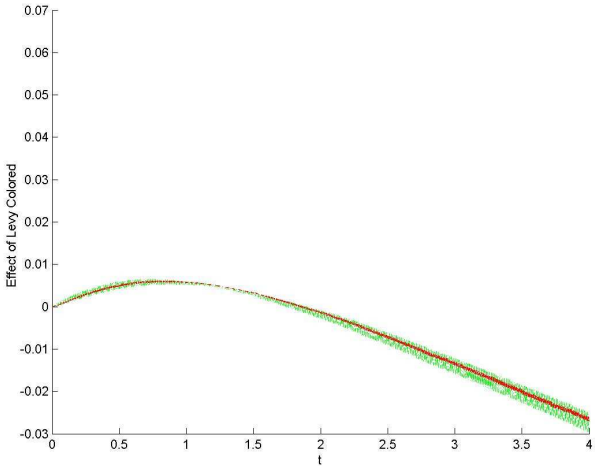


**Figure 15: averaged salinity with Lévy Colored noise - non-homogenous Neumann (base case); $f = 1$ red, $f = 1.5$ yellow, $f = 2$ green**

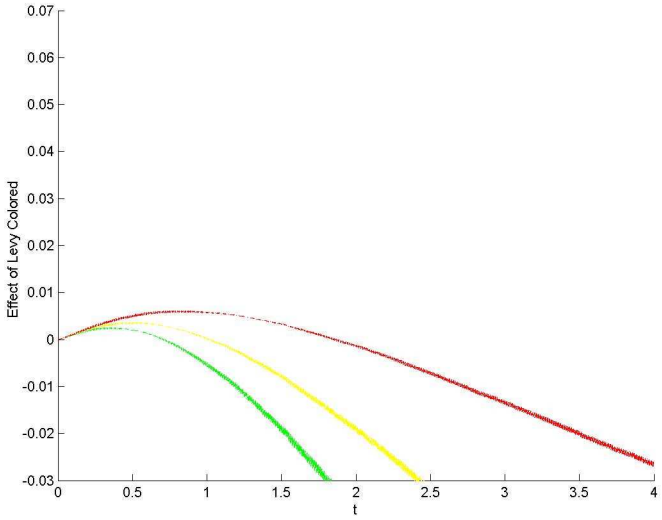


**Figure 16: averaged salinity with Lévy Colored noise - non-homogenous Neumann (base case); $\sigma$=1 red $\sigma$= 1.5 yellow $\sigma$=2 green**

Finally, Wiener white and colored noises as well as Lévy white noise on the boundary help the transport process, but Lévy colored noise eventually suppresses the transport process, and it does so faster as the distribution of the Lévy process gets closer to being Gaussian. The noise effect shows the same resonance-like behavior seen before, as we vary the frequency of the shear flow. Not unexpectedly, the noise effect from Lévy colored noise shows the same sensitivity to the strength of the noise, but is insensitive to all other noises.

# 4. ACKNOWLEDGMENTS

The authors thank the anonymous reviewers for their careful reading of this paper, and their very helpful comments and suggestions. V.P. Boñgolan would like to thank her co-authors for their patience with this paper. It began as unfunded research, was continued under an ERDT Visiting Professor grant at the College of Engineering of the University of the Philippines Diliman (2008-2009), and was completed with the help of the Cesar A. Buenaventura UP Centennial Professorial Chair (2010-2011).

# 5. REFERENCES

[1] Simpson, J. E., 1982: Gravity currents in the laboratory, atmosphere, and the ocean. *Ann. Rev. Fluid Mech.*, **14**, 213-234.

[2] Cenedese, C., J. A. Whitehead, T. A. Ascarelli and M. Ohiwa, 2004: A Dense Current Flowing Down a Sloping Bottom in a Rotating Fluid. *J. Phys. Oceanogr.*, **34**, 188-203.

[3] V.P. Boñgolan-Walsh, J. Duan, P.F. Fischer, T. Özgökmen, and T. Iliescu. "Impact of Boundary Conditions on Entrainment and Transport in Gravity Currents." *Journal of Applied Mathematical Modelling* **31 (7)**:1338-1350, (2007)

[4] V.P. Boñgolan-Walsh, J. Duan, and T. Özgökmen. "Dynamics of Transport under Random Fluxes on the Boundary." *Communications in Nonlinear Science and Numerical Simulation* **13**, (October 2008), 1627-1641.

[5] S.P. Murray, and W.E. Johns, Direct Observations of seasonal exchange throught the Bab el Mandab Strait. *Geophys. Res. Lett.* **24** (1997), 2557-2560.

[6] P.E. Kloeden and E. Platen, *Numerical Solution of Stochastic Differential Equations*, Springer-Verlag, Berlin, 1999.

[7] B. McNamara and K. Wiesenfeld, Theory of Stochastic Resonance.*Pysical Review A* **39, No. 9** (1989), 4854-4869.

[8] W. R. Young, P.B. Rhines and C.J.R. Garrett, Shear-Flow Dispersion, Internal Waves and Horizontal Mixing in the Ocean*Journal of Physical Oceanography* **12** (1982) 515–527.

[9] G. Da Prato and J. Zabczyk,Evolution equations with white-noise boundary conditions. *Stochastics Stochastics Rep.* **42**:167-182, (1993).

[10] A. Janicki and A. Weron, *Simulation and Chaotic Behavior of alpha-Stable Stochastic Processes*, Marcel Dekker, Inc., New York, 1994.

[11] H. Kunita, *Stochastic Differential Equations Based on Lévy Processes and Stochastic Flows of Diffeomorphisms in New Perspectives (Trends in Mathematics)*, M.M. Rao, Ed., Birkhäuser, Berlin, 2004.